JOC Article

Highly Stereospecific Epimerization of α-Amino Acids: Conducted Tour Mechanism

Indrajit Bandyopadhyay,[†] Han Myoung Lee,[†] P. Tarakeshwar,[†] Chunzhi Cui,[†] Kyong Seok Oh,[†] Jik Chin,*[,‡] and Kwang S. Kim*[,†]

National Creative Research Initiative Center for Superfunctional Materials, Department of Chemistry, Division of Molecular and Life Sciences, Pohang University of Science and Technology, San 31, Hyojadong, Pohang 790-784, Korea, and Department of Chemistry, University of Toronto, Toronto, Ontario, Canada M5S 3H6

kim@postech.ac.kr

Received January 30, 2003

The highly stereospecific and regiospecific recognition of α-amino acids exhibited by a novel Co(III) metal complex embodied in the experimental work (*Nature* **1999**, *401*, 254) is rationalized from the energetics and structural characteristics with the use of density functional calculations. The steric repulsion between the chiral center of the receptor [Co(III) complex] and alanine has been a cause for the discrimination of complex stabilities. The energies evaluated for all possible alanine binding modes clearly reveal regiospecificity. Our main emphasis is laid on the base-catalyzed epimerization reaction that drives the stereospecific recognition to near completion. The conducted tour mechanism is found to be the most likely candidate. A similar role by the equivalent Zn(II) complex is found.

Introduction

Chiral recognition is one of the fundamental chemical and biological processes having vast applications such as enzyme selectivity, immunological response, ion transport, etc. Because of the frequent use of the side chains of basic amino acids (e.g., Lys, Arg, His, Ala) for biological processes, the molecular recognition of these amino acids by synthetic receptor molecules has been attracting much attention. Therapeutic drugs are made from chiral amino acids intermediates, which are increasingly required in enantiomerically pure form.[1] Designing rationally efficient receptors for chiral recognition and the subsequent resolution of amino acids mimicking unsurpassed enzyme selectivity is an arduous task.[2] Recently Chin et al. reported a novel chiral Co(III) metal complex, **1**, that binds natural α-amino acids with high and predictable stereospecificity.[3] More surprisingly, in the subsequent reaction of the diastereomeric mixture (**2a** and **2b**) with NaOD in D_2O, the stereospecific recognition is driven to near completion. To fully utilize the strategy for designing more efficient ligands for chiral recognition, a clear understanding of the epimerization mechanism is essential. The efficiency of the equivalent Zn(II) complex ligand vis-à-vis the Co(III) complex is intriguing to explore. Here we elucidate all these issues using the quantum theoretical method with which a wide range of chemical problems have been solved successfully.[4]

Theoretical Basis

The geometries of all the structures (reactants, products, and intermediates for both Co(III) and Zn(II) complexes) were fully optimized by the density functional calculations with Becke three parameters, using the Lee−Yang−Parr functional (B3LYP)[5] employing the 6-31G* basis set. The corresponding relative energies without and with zero-point energy (ZPE) correction are denoted as ΔE_e and ΔE_0, respectively. The single-point energies of the optimized structures were additionally calculated by using the B3LYP method with the 6-311G** basis set for the $-C_\alpha H-C(=O)$ and Na-moiety and 6-31G* for the rest according to the request made by one of the referees. These calculations will be denoted as B3LYP/(6-311G**) and the corresponding relative energies will be designated as $\Delta E_e'$. The energies in the solvent phase (dielectric constant ϵ 78.4) were evaluated by the polarized continuum

* To whom correspondence should be addressed.
[†] Pohang University of Science and Technology.
[‡] University of Toronto.

(1) Collins, A. N.; Sheldrake, G. N.; Crosby, J. *Chirality in Industry*; Wiley and Sons: Chichester, UK, 1992, Vol. 1; 1997, Vol. 2.
(2) (a) Zhang, X. X.; Bradshaw, J. S.; Izatt, R. M. *Chem. Rev.* **1997**, *97*, 3313. (b) Kim, K. S.; Kim, B. H.; Park, W. M.; Cho, S. J.; Mhin, B. J. *J. Am. Chem. Soc.* **1993**, *115*, 7472. (c) Famulok, M.; Szostak, J. W. *J. Am. Chem. Soc.* **1992**, *114*, 3990. (d) Ellington, A. D.; Szostak, J. W. *Nature* **1990**, *346*, 818.
(3) Chin J.; Lee, S. S.; Lee, K. J.; Park, S.; Kim, D. H. *Nature* **1999**, *401*, 254.
(4) (a) Torrent, M.; Vreven, T.; Musaev, D. G.; Morokuma, K.; Farkas, O.; Schlegel, H. B. *J. Am. Chem. Soc.* **2002**, *124*, 192. (b) Sekiguchi, A.; Ishida, Y.; Fukaya, N.; Ichinohe, M.; Takagi, N.; Nagase, S. *J. Am. Chem. Soc.* **2002**, *124*, 1158. (c) Kim, K. S.; Oh, K. S.; Lee, J. Y. *Proc. Natl. Acad. Sci. U.S.A.* **2000**, *97*, 6373. (d) Kim, K. S.; Tarakeshwar, P.; Lee, J. Y. *Chem. Rev* **2001**, *100*, 4145. (e) Hong, B. H.; Bae S. C.; Lee C.-W.; Jeong, S.; Kim, K. S. *Science* **2001**, *294*, 348. (f) Woodcock, H. L.; Moran, D.; Schleyer, P. v. R.; Schaefer, H. F., III *J. Am. Chem. Soc.* **2001**, *123*, 4331. (g) Florian, J.; Leszczynski, J. *J. Am. Chem. Soc.* **1996**, *118*, 3010. (h) Hrovat, D. A.; Chen, J.; Houk, K. N.; Borden, W. T. *J. Am. Chem. Soc.* **2000**, *122*, 7456. (i) Hong, B. H.; Lee, J. Y.; Lee, C.-W.; Kim, J. C.; Bae, S. C.; Kim, K. S. *J. Am. Chem. Soc.* **2001**, *123*, 10748. (j) Kim, K. S. *Bull. Korean Chem. Soc.* **2003**, *24*, 757.
(5) Becke, A. D. *J. Chem. Phys.* **1993**, *98*, 5648.

10.1021/jo034130c CCC: $25.00
Published on Web 08/01/2003

TABLE 1. Geometrical Parameters and Relative Energies of Diastereoisomeric Co(III) (2) and Zn(II) (3) Complexes, the Intermediates (I), and Molecular Complexes (C) at the B3LYP/6-31G* Level [M = Co(III)/Zn(II)][a]

Geometrical Parameters (bond lengths in Å and angles in deg)

	2a	**2b**	**3a**	**3b**
$H_6\cdots C_9$	4.748	3.262	5.129 (5.058)	4.146 (3.118)
$M-N_2$	1.962	1.968	2.191 (2.155)	2.192 (2.156)
$M-O_5$	1.879	1.874	2.012 (2.021)	2.004 (2.010)
$C_7-C_3-H_6-C_4$	−122	121	−121 (−121)	118 (120)
$O_5-M-N_2-C_3$	−19	−7	−30	−18

	2a′	**2b′**	**3a′**	**3b′**
$H_6\cdots C_9$	4.785	3.320	5.127	4.216
$M-O_5$	1.862	1.859	1.975	1.969
$M-N_2$	2.003	2.007	2.251	2.256
$O_5-M-N_2-C_3$	21	6	28.4	16
$N_2-M-O_5-C_4$	−8	−7	−14	−9

Relative Energies (kcal/mol)

2a	**2b**	**2a′**	**2b′**	**3a**	**3b**	**3a′**	**3b′**
0.00 [0.00]	1.05 [0.97]	8.67	9.88	0.00 [0.00]	0.91 [0.42]	6.89	8.16

	2C$_1$	**2T$_1$**	**2I**	**2T$_2$**	**2C$_2$**
ΔE_e	0.00[0.00]	4.31 [7.79]	−4.28 [3.40]	1.25 [4.45]	−15.89 [−13.29]
ΔE_0	0.00	1.28	−4.18	0.85	−15.46
ΔE_0^D	0.00	1.18	−4.38	0.73	−15.70
$\Delta E_e'$	0.00	3.91 [7.45]	−5.80 [1.53]	0.20 [4.32]	−16.90 [−14.01]

	3C$_1$	**3T$_1$**	**3I**	**3T$_2$**	**3C$_2$**
ΔE_e	0.00 [0.00]	14.08 [16.07]	5.96 [8.07]	11.02 [12.49]	−9.79 [−10.74]
ΔE_0	0.00	10.95	5.48	9.36	−9.54
ΔE_0^D	0.00	10.92	5.34	9.55	−9.64
$\Delta E_e'$	0.00 [0.00]	13.62 [18.72]	4.32 [8.32]	10.25 [13.72]	−9.41 [−11.01]

[a] All values are at the B3LYP/6-31G* level except for the structural values in parentheses which are at the MP2/6-31G* level by full geometry optimization and the relative energies $\Delta E_e'$ which are at the B3LYP/(6-311G**) level (see text). The MP2/6-31G* relative energy of **3b** with respect to **3a** is 1.47 kcal/mol, consistent with the B3LYP/6-31G* value (0.91 kcal/mol). The values in brackets are obtained for the water medium (ϵ 78.4). ΔE_e and ΔE_0 (ΔE_0^D includes the deuterium effect) are the relative energies without and with zero-point correction, respectively.

model (PCM).[6] The charge and multiplicity for Co(III) complexes (**2a, 2b, 2a′, 2b′, 2C$_1$, 2T$_1$, 2I, 2T$_2$**, and **2C$_2$**) are +1 and 1, while those for the Zn(II) complexes are 0 and 1. All calculations for reactants, intermediates, molecular complexes, and transition structures were done with Gaussian98.[7] The select geometrical parameters along with the relative energies of all species are presented in Table 1. Our further discussions will be based on B3LYP/6-31G* results unless otherwise specified since B3LYP/(6-311G**) results are found to be similar to the B3LYP/6-31G* results.

Results and Discussion

The structure of diastereoisomer **2a** agrees well with the X-ray data[3] with an average deviation of 0.03 Å in bond lengths, 2 deg for bond angles, and 6 deg in torsional angles (Table 1). Comparison of the geometrical parameters of **2a** and **2b** shows that the largest difference between **2a** and **2b** occurs in the $H_6\cdots C_9$ distance (4.75 vs 3.26 Å). Thus, this structural parameter is responsible for the steric repulsion.[8] This, in turn, accounts for the differences in complex stabilities of the two main products **2a** and **2b**, and thus is responsible for enantiomeric recognition in a thermodynamically controlled reaction. We have investigated the complexes with alanine's O and N sites at equatorial and axial positions, respectively. These configurational isomers are designated as **2a′** and **2b′** for the corresponding stable complexes **2a** and **2b**, respectively (Figure 1). The energies of these complexes are much higher than those of **2a** and **2b** (by ∼10 kcal/mol) due to greater charge repulsion between two highly electronegative axial and equatorial oxygens, thus rationalizing regiospecificity. The calculations on predominant structures **2a** and **2b** show that the energy of the optimized **2a** is slightly lower than that of **2b**. The difference in energies is 1.05 kcal/mol. If the reaction was thermodynamically controlled, the product ratio ($e^{-\Delta E/RT}$) at 298 K would be 0.17. Here it should be noted that the experimental ratio found is approximately 0.3:0.7 ≈ 0.4. In aqueous medium (ϵ 78.4), the relative energy of **2b** is 0.97 kcal/mol, which corresponds to the probability factor

(6) Barone, V.; Cossi, M.; Tomasi, J. *J. Comput. Chem.* **1998**, *19*, 404.

(7) Frisch, M. J.; Trucks, G. W.; Schlegel, H. B.; Scuseria, G. E.; Robb, M. A.; Cheeseman, J. R.; Zakrzewski, V. G.; Montgomery, J. A., Jr.; Stratmann, R. E.; Burant, J. C.; Dapprich, S.; Millam, J. M.; Daniels, A. D.; Kudin, K. N.; Strain, M. C.; Farkas, O.; Tomasi, J.; Barone, V.; Cossi, M.; Cammi, R.; Mennucci, B.; Pomelli, C.; Adamo, C.; Clifford, S.; Ochterski, J.; Petersson, G. A.; Ayala, P. Y.; Cui, Q.; Morokuma, K.; Malick, D. K.; Rabuck, A. D.; Raghavachari, K.; Foresman, J. B.; Cioslowski, J.; Ortiz, J. V.; Stefanov, B. B.; Liu, G.; Liashenko, A.; Piskorz, P.; Komaromi, I.; Gomperts, R.; Martin, R. L.; Fox, D. J.; Keith, T.; Al-Laham, M. A.; Peng, C. Y.; Nanayakkara, A.; Gonzalez, C.; Challacombe, M.; Gill, P. M. W.; Johnson, B.; Chen, W.; Wong, M. W.; Andres, J. L.; Gonzalez, C.; Head-Gordon, M.; Replogle, E. S.; Pople, J. A. *Gaussian 98*, Revision A.5; Gaussian, Inc.: Pittsburgh, PA, 2001.

(8) The interaction energy between $-C_\alpha HMe$ and $-NMe_2$ moieties in **2b** was analyzed by B3LYP/6-31G* calculations, using the moieties H_3C-Me and $HNMe_2$ of the **2b** geometry. The energy was found to be repulsive by 0.50 ± 0.25 kcal/mol where 0.25 kcal/mol is half the basis set superposition correction.[4d]

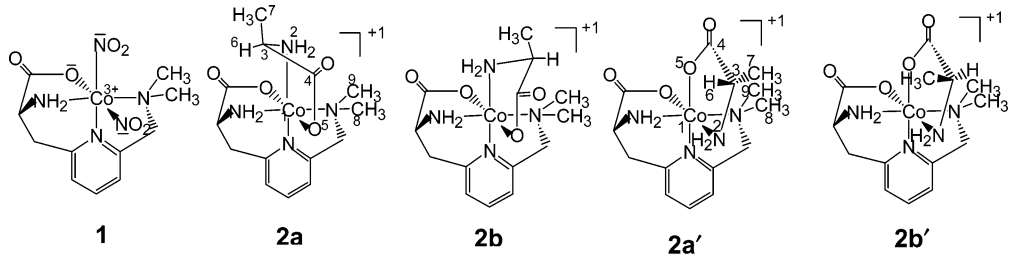

FIGURE 1. Structures of the chiral cobalt complex (**1**), the alanine-bound chiral cobalt complexes (**2a**,**2b**), and their regioisomers (**2a′**,**2b′**).

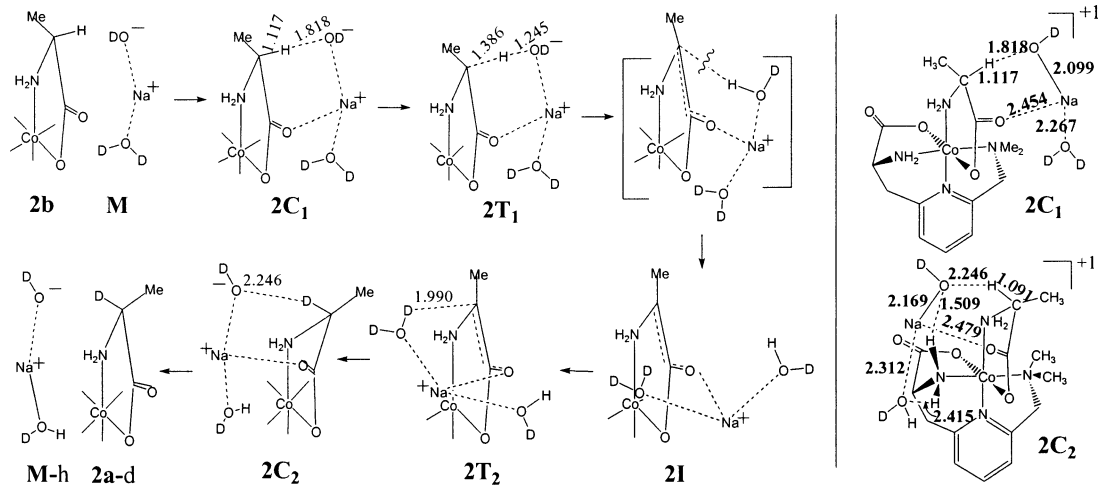

FIGURE 2. Schematic structural transformation in the conducted tour mechanism (B3LYP/6-31G* level).

0.19, showing a slight suppression of enantiomeric recognition for a thermodynamically controlled reaction.

However, when the diastereomeric mixture of **2a** and **2b** is treated with NaOD in D_2O, **2b** epimerizes to **2a** with near completion as revealed by ^1H NMR experiments.[3] The doublet peak of the methyl group of alanine at the stereogenic center [α-C of alanine moiety] for **2a** rapidly changed to the singlet of **2a**-d, while the corresponding doublet peak for **2b** decreased comparatively slowly with the enhanced peak for the **2a**-d methyl group but without the peak for the **2b**-d methyl group. The pathway, known as the "conducted tour mechanism", proposed by Cram et al. for the racemization exchange reaction of 2-methyl-2,3-dihydrobenzothiophene 1-dioxide, 2-(*N*,*N*-dimethylcarboxamido)-9-methylfluorene, and other substrates is helpful in explaining this epimerization.[9] In this mechanism, the aqua-sodium hydroxide ($NaOD(D_2O)$), which will be denoted as **M**, detaches a proton from $\mathbf{2C_1}$ to form a sodium carbanide ion pair via the first transition state ($\mathbf{2T_1}$). Then, an intermediate state (denoted as **2I,** where carbanionic charge is delocalized over C and carbonyl O) is formed. By barrierless rotation of the moiety, the conjugate acid of the catalyst migrates to the back face of the carbanion. Reorganization produces $\mathbf{2C_2}$ after passing the second transition state ($\mathbf{2T_2}$), where the sodium hydroxide moiety has migrated to the back face of the carbanion (vide Figure 2). Thus, the scheme of the reaction pathway is as follows: $\mathbf{2b} + \mathbf{M} \rightarrow \mathbf{2C_1} \rightarrow \mathbf{2T_1} \rightarrow \mathbf{2I} \rightarrow \mathbf{2T_2} \rightarrow \mathbf{2C_2} \rightarrow$ **2a**-d + **M**-h, where **2a**-d and **M**-h denote deuterated **2a** and $NaOH(D_2O)$, respectively. The transition structures were confirmed by the existence of imaginary frequencies at

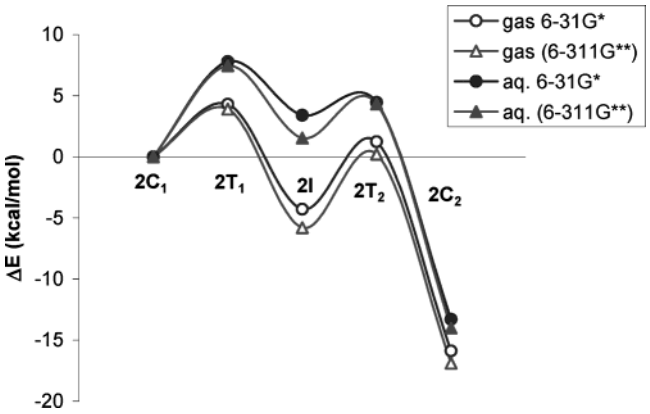

FIGURE 3. Potential energy profile in the conducted tour mechanism for interconversion of **2a** and **2b** in the gas phase and aqueous (ϵ 78.49) reaction profiles (○, Δ: B3LYP/6-31G*; ●, ▲: B3LYP/(6-311G**)).

the B3LYP/6-31G* level (996.6i cm^{-1} for $\mathbf{2T_1}$; 42.6i cm^{-1} for $\mathbf{2T_2}$; for corresponding deuterated species 992.9i cm^{-1} and 42.5i cm^{-1}, respectively). The normal coordinate motions corresponding to the imaginary frequencies show that they follow the reaction coordinate.

The energy profiles of the mechanism in the gas and aqueous phases are shown in Figure 3. The overall reaction from **2b** to **2a**-d is exothermic. The large energy difference between two states ($\mathbf{2C_1}$, $\mathbf{2C_2}$) arises from formation of additional H-bonds between the amine group and one water adjacent to the Co and between the hydroxyl oxygen and the amine hydrogen in the case of $\mathbf{2C_2}$. For the condensed phase, attempts were made to

obtain results excluding the two H-bond effects by conducting supermolecular calculations on H_2O-NH_3 and $NaOH-NH_3$ complexes. Excluding these extra intracomplex H-bond energies in **2C₂**, the relative stability of **2C₂** over **2C₁** is 1.03 (i.e. 15.89 − 14.86) kcal/mol (Table 1). The barrier height for deprotonation of **2C₁** is 4.31 kcal/mol; the reorganization barrier for **2I** is 5.53 kcal/mol. In D_2O, these values are 7.79 and 1.05 kcal/mol, respectively. The gaps between **2T₁** and **2T₂** states (the transition state selectivity, $\Delta\Delta E^{\ddagger}$) are 3.06 kcal/mol in the gas phase and 3.34 kcal/mol in D_2O, which are in good agreement with the experimental $\Delta\Delta G^{\ddagger}$ (2.8 kcal/mol) obtained from global forward and backward rate constants. Thus, the kinetic conversion from bound L-alanine to bound D-alanine is readily accomplished almost completely. It is to be noted that the results for $\Delta E_e'$ [i.e. B3LYP/(6-311G**)] presented in Table 1 and Figure 3 are similar.

One might think that the formation of **2a**-d from **2b** could be explained by two other possible pathways. One is the kinetically analogous DO^--catalyzed carbanion mediated mechanism. This mechanism was also proposed for a plethora of related reactions.[10] For, e.g., mutarotation of coordinated amino acid, valine was shown by NMR and polarimetric equilibration studies of the D-[$Co(en)_2$-L-(val)]Cl_2 complex. The kinetic studies revealed that the rate of proton exchange as well as mutarotation is given by Rate = k[Co][OH^-]. Thus the carbanion (enolate)-mediated mechanism was proposed that explains the rate equation. This mechanism has been controversial as it involves the initial generation of enolate as an intermediate. However, the mechanism in the present system seems unlikely because of the large instability of the carbanion intermediate with respect to the reactants.

Thus the energy available to the system is too small to initiate the reaction making the formation of the anionic intermediate a thermodynamically (and therefore kinetically) unfavorable process. It has to be noted that there were studies to reduce the instability by various stabilizing factors.[11] Still the results rule out the possibility of generation of the carbanion in the reaction conditions. It is to be noted that there are no spectroscopic or other evidence for enolates. The other mechanism is the intramolecular enol-mediated mechanism.[12] This mechanism along with the energy profile is shown in Figure 4. Again, in this case, the relatively higher activation barrier makes the mechanism less likely compared to the conducted tour mechanism. Furthermore, the intermediate was not observed in the experiment, indicating that the reaction mechanism did not operate because of a high activation barrier. The conclusions are still valid for the B3LYP/(6-311G**) calculations (see Figure 4).

The efficiency of the equivalent Zn(II) ligand vis-à-vis the Co(III) ligand (i.e., **3** vs **2**) is investigated. Comparison

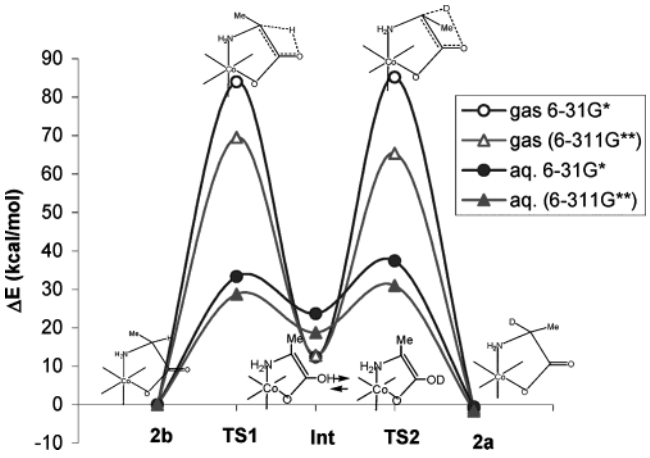

FIGURE 4. Potential energy profile in the intramolecular enol-mediated mechanism for co-isomerization of **2a** and **2b** in the gas phase and aqueous (D_2O, ϵ 78.49) reaction profiles (○, Δ: B3LYP/6-31G*; ●, ▲: B3LYP/(6-311G**)).

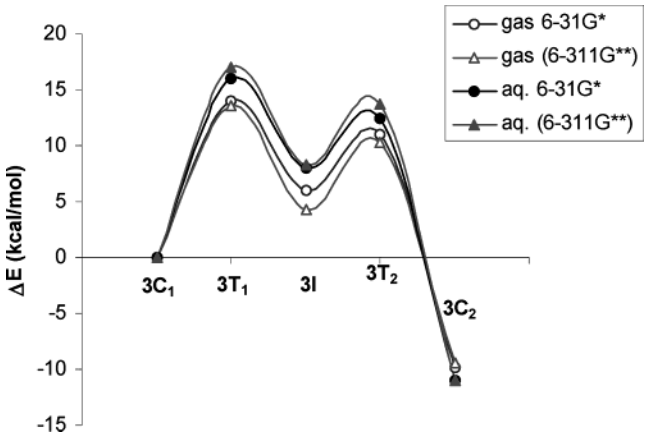

FIGURE 5. Gas-phase reaction energy pathway in the conducted tour mechanism for the interconversion of analogous Zn(II) complexes, **3a** and **3b** (○, Δ: B3LYP/6-31G*; ●, ▲: (B3LYP/6-311G**)).

of the geometrical parameters shows that the largest difference between **3a** and **3b** occurs in the $H_6\cdots C_9$ distance (5.13 vs 4.22 Å). The variation in this structural parameter, responsible for the variation in steric repulsion,[8] would account for the differences in complex stabilities of the two main products **3a** and **3b**, thus for the enantiomeric recognition in a thermodynamically controlled reaction. The calculations further reveal that the energy of the optimized **3a** is lower than that of **3b** (0.91 kcal/mol). This energy difference could account for the stereospecificity. The corresponding Boltzmann probability factor at 298 K is 0.21. The energies of the configurational isomeric complexes **3a′** and **3b′** (which are equivalent to **2a′** and **2b′**, respectively) are much higher compared to those of **3a** and **3b**, showing regiospecific recognition by the Zn(II) ligand. The transition state structure calculations show that the activation barrier for deprotonation of **3C₁** is 14.08 kcal/mol; the reorganization barrier for **3I** is 5.06 kcal/mol. In D_2O, these values are 16.07 and 4.43 kcal/mol, respectively. Both the transition structures were confirmed by the existence of one imaginary frequency for each structure at the B3LYP/6-31G* level (104.4i cm^{-1} for **3T₁**; 49.7i

(9) (a) Cram, D. J.; Whitney, T. A. *J. Am. Chem. Soc.* **1967**, *89*, 4651. (b) Ford, W. T.; Cram, D. J. *J. Am. Chem. Soc.* **1968**, *90*, 2606.

(10) (a) Buckingham, D. A.; Marzilli, L. G.; Sargeson, A. M. *J. Am. Chem. Soc.* **1967**, *89*, 5133. (b) Zelewski, A. *Stereochemistry of Coordination compounds*; Wiley and Sons: Chichester, UK, 1996; p 211.

(11) Zheng, Y.-J.; Bruice, T. C. *J. Am. Chem. Soc.* **1997**, *119*, 8137.

(12) See, for example: Streitweiser, A.; Heathcock, C. H.; Kosower, E. M. *Introduction to Organic Chemistry*; Macmillon: New York, 1992; p 430.

cm^{-1} for $\mathbf{3T_2}$; for corresponding deuterated species the values are 102.0i and 48.9i cm^{-1}, respectively). Similar to Co(III), the transition state selectivity is 3.06 (in D_2O 3.57 kcal/mol) kcal/mol. The results for ***3*** are presented in Table 1 and Figure 5. Thus, the Zn(II) receptor can be profitably utilized for epimerization of α-amino acids.

Conclusions

In summary, we have studied the Co(III) complex binding alanine with high stereo- and regiospecificity, using ab initio methods. Our results are in good agreement with the experimental observations. It is found that the chiral discrimination is determined by steric repulsion in terms of reactant and product energetics. However, the main attention was focused on the base-catalyzed epimerization, which drives the chiral recognition to near completion because of the large difference in forward and reverse transition barriers from the intermediate state. The most plausible reaction pathway for the epimerization is found to be the "conducted tour mechanism" among three mechanistic pathways. The structures and energies of all the intermediates, molecular complexes, and transition states were calculated. The energy profile for the transformation **2b** → **2a**-d was obtained. The Zn(II) complex receptor also shows considerable chiral recognition toward alanine. The present study will help design new receptors for epimerization-driven chiral recognition of α-amino acids and other related compounds, and also help understand several related reactions.

Acknowledgment. This study was supported by MOST-(KISTEP)/CRI and BK21. Most of calculations were performed with supercomputers at KISTI, Korea.

Supporting Information Available: Cartesian coordinates and energies of optimized geometries in Figure 1; free energy profiles (Figure S1). This material is available free of charge via the Internet at http://pubs.acs.org.

JO034130C